行政院國家科學委員會專題研究計畫　期中進度報告

量子奈米導線之新穎物理性質之研究(1/3)

計畫類別：個別型計畫
計畫編號：NSC93-2120-M-009-009-
執行期間：93 年 08 月 01 日至 94 年 07 月 31 日
執行單位：國立交通大學電子物理學系(所)

計畫主持人：林志忠
共同主持人：簡紋濱，開執中，陳福榮，吳玉書
計畫參與人員：邱劭斌、歐逸青、韓顏吉、葉佳唯、潘正達、蔡錦盛、廖家慶、莊惠芳、李秉奇

報告類型：精簡報告

處理方式：本計畫可公開查詢

中　華　民　國 94 年 5 月 27 日

摘要

在本（第一年度）進度中，我們合成金屬氧化物、半導體、及高溫超導體等各式量子奈米導線，並研究其晶格結構特性、磁性質、和低溫電子傳輸性質。本計畫充分發揮奈米科技研究的跨領域特性，緊密的結合了材料合成、超高解析穿透式電子顯微術（HRTEM）、高精密低溫電子傳輸量測技術、低溫掃瞄探針顯微術，和 SQUID 技術等，從樣品製作到物性量測，再到數據分析與計算，環環相扣，進展順利。

在這第一年度（2004 年 8 月至 2005 年 7 月）中，我們具體完成了以下工作：（一）成功的成長出不同直徑的各式氧化物奈米線，同時利用HRTEM技術，決定其晶格結構。又運用Electron Energy Loss Spectroscopy（EELS）技術，檢測電漿損失能譜的尺寸效應。（二）成功的運用電子束蝕刻技術（electron beam lithography），製作出極低接點阻抗（contact resistance）的四點次微米金屬電極。（三）成功的將奈米線的四點電性（電阻、磁電阻、電流-電壓特性曲線）量測，推展到液氦的溫度。（四）成功的量測出稀磁半導體奈米線的鐵磁特性，退火效應，並釐清形成其鐵磁性質的物理機制。同時，我們進行了兩項尖端奈米量測技術的開發：（一）STM/TEM單根奈米線電性量測技術，和（二）低溫掃瞄探針顯微鏡的設立。

關鍵詞：量子奈米導線、超高解析穿透式電子顯微術、低溫電子傳輸、稀磁半導體奈米線、低溫掃瞄探針顯微術

Abstract

In this first year of our Quantum Nanowire project, we have accomplished the following tasks. (1) We have successfully grown several kinds of nanowires, including metal oxide, semiconductor, and high-temperature superconductor nanowires. We have performed HRTEM studies of the crystal structures on the nanowires. The dependence of plasma frequency on the diameter of nanowires has been investigated, using Electron Energy Loss Spectroscopy. (2) Utilizing electron-beam lithography technique, we have successfully fabricated sub-micron electrodes onto the nanowires. The contact resistances are very low and highly reproducible. (3) We have achieved four-probe measurements of the resistances, magnetoresistances, and current-voltage characteristics on the nanowires down to liquid-helium temperatures. The intrinsic electrical-transport properties of various nanowires have been studied. (4) We have performed magnetic property measurements on diluted-magnetic semiconductor nanowires. The correlation between thermal annealing conditions, crystal structures, and the magnetic properties are clarified. In addition, we have developed and set up two novel systems for nanowire measurements: (1) an STM/TEM system for conductance measurements on individual nanowires, and (2) a low-temperature scanning probe microscope.

Keywords: quantum nanowires, HRTEM, low-temperature electrical-transport properties, ferromagnetic properties, low-temperature scanning probe microscopy

報告內容

本項奈米國家型計畫的執行期限為自 2004 年 8 月 1 日至 2007 年 7 月 31 日止，共三年，今年為第一執行年度。在近一年的執行期間，本計畫的主要進度和成效包括：（一）氧化物奈米線之成長與晶格結構分析，（二）單根氧化物奈米線之本徵電性量測，（三）稀磁半導體奈米線之鐵磁量測及性質研究，（四）奈米線電漿損失能譜之量測，（五）奈米線量測技術之開發：STM/TEM電性量測技術，和（六）奈米線量測技術之開發：低溫掃瞄探針顯微術等六項。茲詳細說明如下。

（一）氧化物奈米線之成長與晶格結構分析

我們利用物理/化學氣相傳輸法成長了各種氧化物奈米導線，並進一步探討奈米尺度下的新穎物性。採用氧化物奈米線的最主要原因在於，在常溫和常壓下，這類奈米線較為穩定，不再產生進一步的相變化和氧化。物理/化學氣相傳輸法是目前成長奈米線之最普遍的一種製程方式，主要是利用高溫將原料加熱汽化或分解，並藉由載氣將反應氣體輸送到低溫處，透過Vapor-Solid或是Vapor-Liquid-Solid等成長機制製備奈米線。目前本計畫已經成長的導電或半導體奈米線計有RuO_2,、ITO、ZnO、$Zn_{1-x}Co_xO$、和高溫超導體$YBa_2Cu_3O_{7-\delta}$奈米線等。在$Zn_{1-x}Co_xO$奈米線中，Co原子乃是藉由implantation的方法打入ZnO奈米線中。我們成長之奈米線的長度大約是 1-5 μm，直徑大約由數nm至 100 nm左右。

在成長完畢之後，進行物理性質量測之前，所有奈米線的晶格結構和成份，都先以高分辨電子顯微鏡以及x-光能譜儀進行分析和確認。例如下面三圖（由左至右）分別為RuO_2奈米線之SEM，HRTEM，以及x-光能譜。這些圖顯示，在這第一個計畫執行年度中，我們已經掌握了各式奈米線的成長技術，並且能夠對成長後的奈米線進行深入而精細的結構和成分分析。

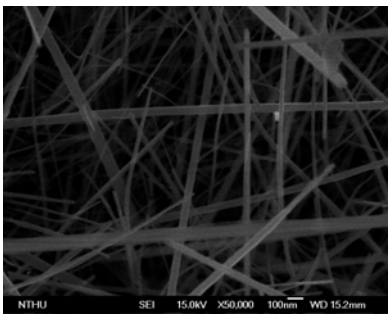

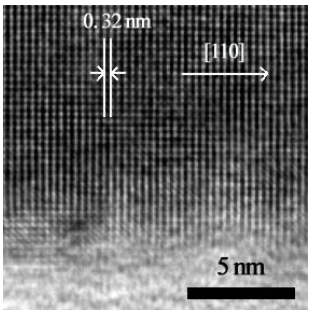

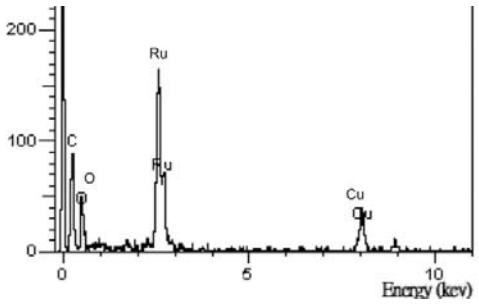

（二）單根氧化物奈米線之本徵電性量測

本項奈米計畫的重點之一，是探討奈米線的本徵電性，與基礎（低溫下接近基態時的）物理特性。欲對奈米線進行本徵電性量測，次微米金屬（如 Au/Ti 或 Au/Cr）電極的製作極為重要，因此掌握電子束蝕刻技術（electron-beam lithography）是最關鍵的首要步驟。經過將近一年的努力，我們對金屬電極的製作技術已經非常嫻熟而能夠確實掌握。在一般情況下，我們可以製作出小於 0.2 μm 寬的金屬電極。更重要的是，我們的次微米

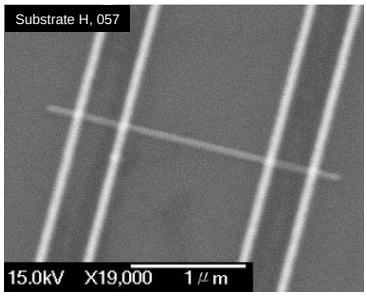

金屬電極與半導體（如 ZnO）奈米線的接點電阻（contact resistance）可以低到數 kΩ；次微米金屬電極與金屬（如 IrO_2）奈米線的接點電阻則更可以低到 100 Ω 以下。右上圖顯示一根 ZnO 奈米線與四根次微米 Au/Ti 電極的漂亮結構。（四根金屬電極係蒸鍍在 ZnO 奈米線上方，而奈米線則平躺在經過氧化處理之 Si wafer 上。）

欲探討奈米線的本徵電性，本項奈米計畫的主要目標在於**四點量測**。經過了長年累積的基礎，再加上最近一年的努力，目前我們已經深入掌握了這些技能。除了次微米金屬電極的製作技術之外，我們對於小電流（~nA）和小電壓的量測技術和解析，都已臻成熟。以較為困難的半導體奈米線的電性量測為例，下二圖顯示一根 ZnO 奈米線的本徵電阻對溫度的變化情形，即四點量測的結果。這是文獻中從未曾報導過的包含最大（左下圖）又最低（右下圖）溫度範圍的成功量測結果。我們預期這一組數據，將成為探討 ZnO 奈米線的本徵電性的重要參考資料。（右下圖中顯示，在 2 K 以下，電阻對溫度的變化呈現出電子-電子交互作用效應的結果。）在接下來的第二執行年度中，我們將針對不同直徑的各式奈米線進行量測，並且探討外加磁場的效應。

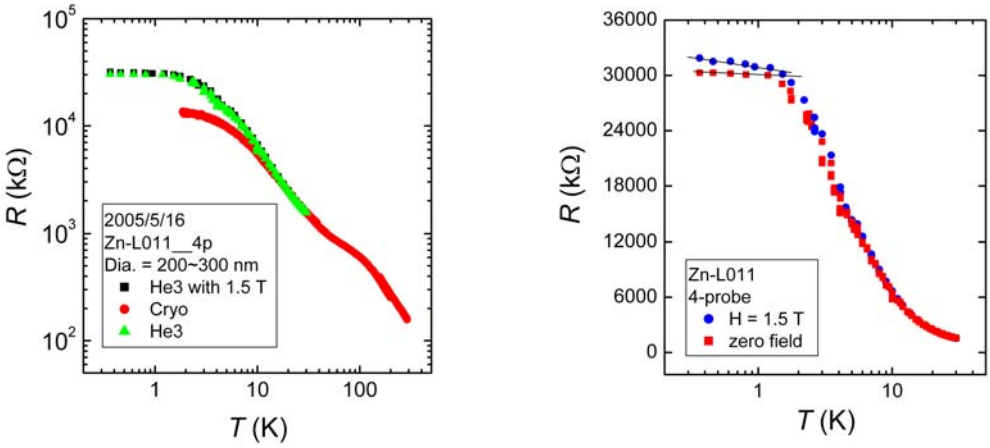

除了對於半導體奈米線的研究，本計畫也針對金屬氧化物奈米線（如 RuO_2、IrO_2、tin-doped indium oxide 即 ITO）進行了量測。由於篇幅有限，而且因為金屬奈米線的量測技術比半導體奈米線的量測技術相對簡易，因此在本期中報告中暫不討論金屬奈米線的結果。（從奈米科學方面說，則金屬奈米線物理可能比半導體奈米線物理更為有趣。）

<u>奈米尺度下金屬-半導體接點之電流-電壓特性曲線研究</u>： 雖然四點量測是研究奈米線之本徵電阻的必要手段，兩點量測則可以用來探討金屬/半導體奈米線介面的特性。充分瞭解半導體奈米線與次微米金屬電極之間的介面行為，是發展奈米電子元件的先遣重要課題。在本計畫的第一年度裡，我們成功的藉由改變ZnO奈米線與Au/Ti電極的接點電阻，來調控兩點量測的電流-電壓特性曲線行為。我們發現當室溫接點電阻小於 100 kΩ 時，ZnO 奈米線與金屬電極所產生之奈米接點的電流-電壓特性呈現飽和電流之曲線圖（即類似於MOSFET的行為），且在同樣溫度小電壓下，其電流值較大（左下圖），此結果可以歸因於穿隧電流的貢獻。當室溫接點電阻大於 100 kΩ 時，其電流-電壓曲線轉為類似*P-N*結之特性曲線（右下圖），此結果可以歸因於熱電流的貢獻。在第二年度中，我們擬藉由控制奈米線/次微米金屬電極之接點的絕緣程度（即接點電阻的大小），從而以bottom-up的方式，做出奈米尺度的*P-N*結或MOSFET等半導體元件。

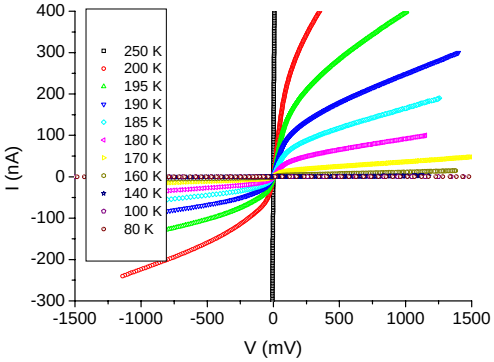

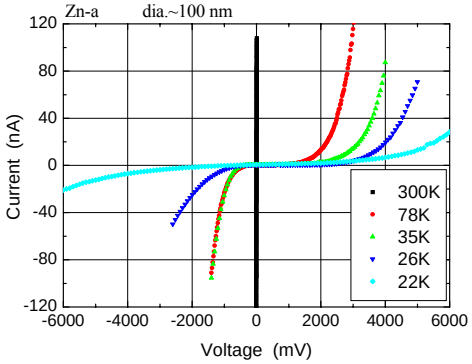

（三）稀磁半導體奈米線之鐵磁量測及性質研究

本年度中，我們進行了以下兩項之稀磁半導體 $Zn_{1-x}Co_xO$ 奈米線的鐵磁性質研究。（一）利用 HRTEM 與 SQUID 技術，我們觀察到在一大氣壓之氫氣中退火後，$Zn_{1-x}Co_xO$ 奈米線之晶格結構變得更為有序（在剛經過高能量的 Co 佈植之後，晶格原子面間含有極多的缺陷），而鐵磁性明顯增強，從而驗證了稀磁半導體中之 carrier-mediated ferromagnetism 的理論概念與物理機制。本項工作細節見附錄一，已投稿至 Applied Physics Letter，克在審查中。

（二）我們探討經**高真空退火**所導致的鐵磁性質變化： 我們發現高真空（10^{-5} torr）退火，除了使晶格結構變得更為有序之外，也造成 ZnO 奈米線中氧缺陷的增加，從而提高了載子濃度，更進而導致鐵磁性的大幅度增強。為了確認所觀測到的強鐵磁性並不是由 Co 叢集（clusters）所造成，我們利用 x-光繞射圖（左下圖）確認在 ≥ 10 nm 大小範圍內，沒有 Co 的第二相產生。我們又從電子能量損失譜（EELS）圖，確認在 ≥ 2 nm 大小範圍內沒有第二相。我們更再從 HRTEM 影像圖中，確定完全沒有 ≥ 1 nm 之 Co 的叢集相。因此，結合多項結構研究的專長之後，我們可以相當肯定，退火前後之鐵磁性強弱的改變，並非由 Co 叢集所造成。右下圖顯示，經高真空退火後，$Zn_{1-x}Co_xO$ 奈米線中的磁滯曲線變得非常明顯。這是由於 *n*-type 載子濃度增加（由氧缺陷造成），因而增強了 Co 離子間的 exchange interaction 所造成的結果。這項實驗顯示，增加載子濃度是提升鐵磁相變溫度的主要原因，與理論預測相符。這一部分的結果，即將投稿至 Journal of Applied Physics，因篇幅較長，僅將摘要列於附錄二。

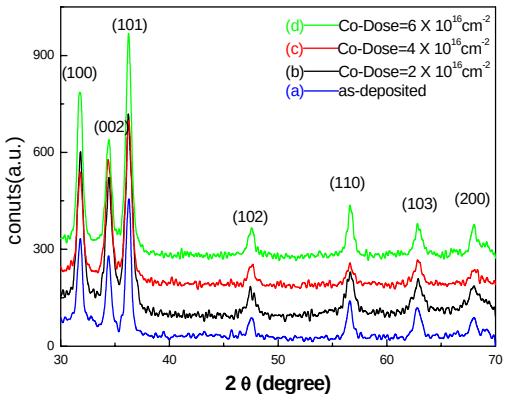

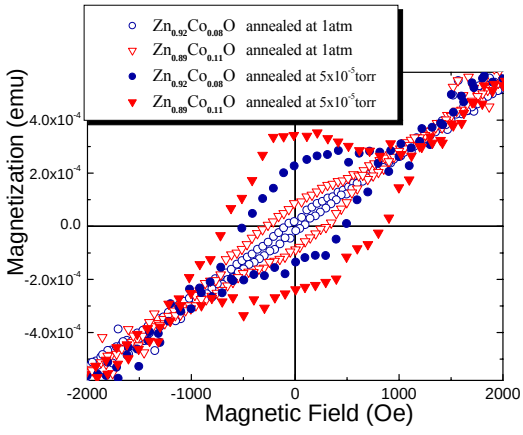

（四）奈米線電漿損失能譜之量測

隨著樣品尺度的減小，在奈米線中其材料特性應與塊材的物性不同。在今年的進度中，我們也對ZnO和RuO_2 兩種奈米線的電漿損失能譜進行了研究。運用EELS的實驗方法，我們量測了不同直徑的單根奈米線的電漿損失能譜。我們發現，ZnO奈米線與RuO_2 奈米線表現出類似的行為。我們的RuO_2 奈米線的初步量測結果，呈現於下面二圖中。左下圖畫出奈米線的電漿能量損失能譜，右下圖畫出奈米線電漿能量偏移量與奈米線直徑（20-125 nm）的關係。由右下圖中可以看出，當奈米線的直徑約大於 60 nm 時，電漿峰值近於 30 eV，此值與單晶RuO_2塊材的電漿峰值相符。值得注意的是，當RuO_2奈米線的直徑約小於 50 nm 時，電漿峰值隨著直徑之減小而迅速增加，表現出明顯的尺寸效應。在 20 nm直徑的奈米線中，電漿峰值增至 33.5 eV。

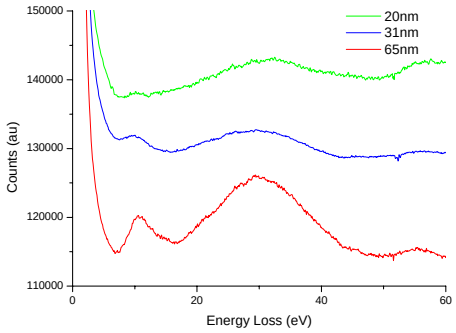

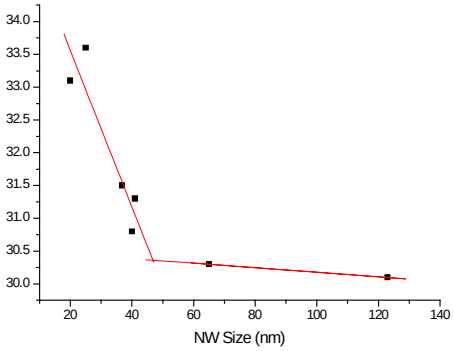

目前我們正分兩個方向進行這方面的研究：（一）經由理論計算，瞭解電漿損失與奈米線尺寸之關係。初步的想法認為，電漿峰值應與奈米線直徑的平方成反比，但需再進一步確認。（二）有系統的量測電漿損失能譜和 STM/TEM 電阻率（請見下節之討論）對各種奈米線之尺寸關係。由於電漿峰值與載子的濃度有關， 這一方向的研究，爾後將與電性傳輸性質的研究相互結合，從而更全面的瞭解奈米導線之物性。

（五）奈米線量測技術之開發：STM/TEM電性量測技術

如上所述，本計畫以電子束蝕刻技術法製作次微米的金屬電極，進行大溫度範圍和磁場中的四點量測，以探討奈米線的本徵電性和低溫下的量子傳輸行為。為了對奈米系統進行更為全面的研究，本計畫也積極開發STM/TEM電性量測技術。所謂STM/TEM電性量測技術是在TEM的樣品台上加裝STM，將單根奈米線的一端接地，STM端則加上正電壓後，量測通過奈米線的電流。左下圖中，顯示一單根奈米線與STM探針。STM/TEM技術提供了一個高空間解析度的直接電性（電流-電壓特性曲線）量測法，但是這種技術是在室溫之下的兩點電性量測，所量到的電阻包含了奈米線本身和STM探針與奈米線之間的接點電阻。所幸STM探針與奈米線之間的接點電阻，可以藉由量測同一跟奈米線的不同長度（沿軸長）處的電阻後加以去除（右下圖）。以RuO_2奈米線為例，運用這個方法，我們初步量得室溫電阻率為 ~210 μΩ cm。這個電阻率，比單晶RuO_2塊材的電阻率（~ 35 μΩ cm）大了約 6 倍，我們覺得是由於奈米線表面氧的計量缺陷所造成的。在第二年度中，我們將有系統的量測電阻率與奈米線直徑的關係，並且探討氧計量缺陷的影響。

$$R_{measured} = R_{wire} + R_{contact}$$

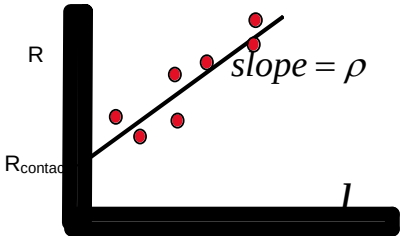

第二年度的計畫，更形重要。我們將設計和製造可控溫度的低溫STM/TEM樣品台，以達到遠低於室溫以下（液氮或液氦）的溫度。這項實驗中最困難的工作之一，在於如何製備非常乾淨的STM探針。我們預計發展探針電解系統（如左下圖所示），並結合Focused Ion Beam的功能，將探針（如Au）的尖端直接銷至 0.1 μm以下（右下圖顯示我們最近的一個例子）。

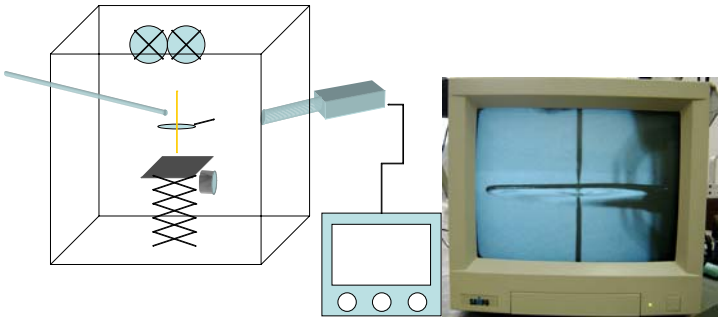

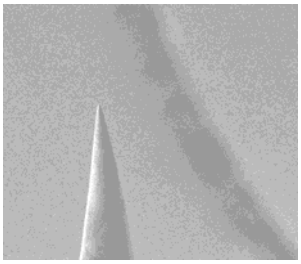

同時，我們將建立真空烘烤系統（如左下圖），以確保探針表面與奈米線能夠保有乾淨的介面。倘使探針的表面不乾淨，將造成失真之接點電阻（如右下圖所示）。

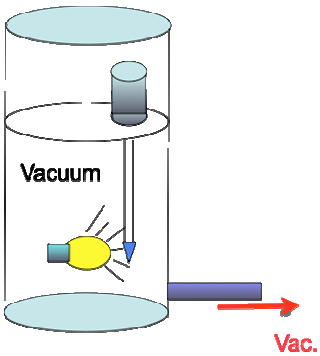

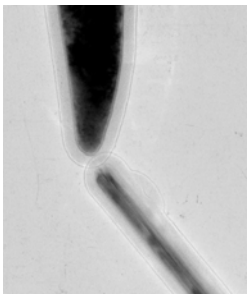

（六）奈米線量測技術之開發：低溫掃瞄探針顯微術

本項奈米計畫的第一年度設備費，全部用以採購一套低溫掃瞄探針顯微鏡。經過與國內、外的一些尖端奈米實驗室請教、討論，並且詳細蒐集資料和仔細評估之後，我們選擇了德國 Omicron 公司製造之 Low Temperature UHV STM System。(最低溫度為 5 K，真空度高達

10^{-11} mbar。）本項設備我們於去年暑假前即已經開始進行評估與設計作業，並且在計畫一經核定之後，即刻與廠商聯繫及協商，迅速完成設計和採購程序。因此本項極為精密的儀器系統，已經於今年四月底前運抵交大，並且原廠工程師此刻正在我們實驗室中進行安裝，預定於本星期完成安裝以及試機。這個進度，令人滿意。預估在幾個月之內，我們就可以對奈米線進行量測，並且攫取得有意義的數據。預定在明年度的期中進度報告中，我們就會有這一方面的數據可以呈現。

因為歐元一直漲價，雖與儀器商再三討論，這套儀器系統售價仍接近台幣 1500 萬元。去年度本計畫獲得的 900 萬元之儀器設備費，全部用以採購本套設備，但仍積欠數百萬元，今年度懇請惠予繼續補助（足）。

計畫成果自評

在執行本項奈米國家型科技計畫的這第一年度（2004 年 8 月至 2005 年 7 月）中，我們密切結合了各項奈米科技的專長，完成了以下工作：（一）由陳福榮及開執中教授領導，成功的成長出不同直徑的各式氧化物奈米線，同時利用 HRTEM 技術，進行其晶格結構量測；並運用 EELS 技術，量測出電漿損失能譜的尺寸變化關係。又成功的將 Co 原子以 implantation 的方式，佈植到 ZnO 半導體奈米線中，從而製作出稀磁半導體並產生鐵磁特性。（二）由林志忠教授領導，成功的運用電子束蝕刻技術，製作出四點次微米金屬電極。同時，把金屬電極與半導體奈米線之間的室溫接點電阻降低到數 kΩ 以下。更將金屬電極與金屬奈米線之間的接點電阻，降低到 100 Ω 以下。（三）由林志忠教授領導，成功的將奈米線的四點電性（電阻、磁電阻、電流-電壓特性曲線）量測，推展到液氦的溫度。（四）由簡紋濱教授領導，成功的量測出稀磁半導體奈米線的鐵磁特性，退火效應，並釐清形成鐵磁性質的物理機制。以上這些結果，即將可以發表。

在本年度中，我們又進行下列兩項尖端奈米技術之開發：（一）STM/TEM 單根奈米線電性量測技術，和（二）低溫掃瞄探針顯微術的設立。這兩項前沿奈米線量測技術的迅速開發完成，將使我們團隊的研究能量更上層樓，對奈米國家型計畫作出更大的貢獻。

附錄一： (Appl. Phys. Lett., submitted)

Structure effects on ferromagnetism in $Zn_{1-x}Co_xO$ nanowires

W. B. Jian*
Department of Electrophysics, National Chiao Tung University, Hsinchu 300, Taiwan, ROC

Z. Y. Wu, R. T. Huang, F. R. Chen, and J. J. Kai
Department of Engineering and System Science, National Tsing Hua University, Hsinchu 300, Taiwan, ROC

C. Y. Wu
Opto-Electronics and Systems Laboratories, Industrial Technology Research Institute, Hsinchu 310, Taiwan, ROC

S. J. Chiang and M. D. Lan
Department of Physics, National Chung Hsing University, Taichung 402, Taiwan ROC

J. J. Lin*
Department of Electrophysics and Institute of Physics,
National Chiao Tung University, Hsinchu 300, Taiwan, ROC

Diameter controllable crystalline ZnO nanowires, with the [0001] growth direction in the plane, have been fabricated by using the thermal evaporation method. The as-grown nanowires with diameter of $\sim$ 40 nm were implanted with various amounts of Co ions. The as-implanted $Zn_{1-x}Co_xO$ ($x \leq 0.11$) nanowires exhibited paramagnetic, but not ferromagnetic, behavior, and possessed high density of radiation induced orientation variations and stacking faults. After annealing the structural defects largely disappeared, and noticeable hysteresis in the magnetization loops revealed apparent ferromagnetic ordering in the nanowires. This work supports the idea of carrier-mediated ferromagnetism in diluted magnetic semiconductors having a long transport mean free path.

Not only high Curie temperature but also the mechanism of carrier-induced ferromagnetism in diluted magnetic semiconductors (DMS) has recently drawn much experimental and theoretical attention. It has been proposed that the ferromagnetism in III-V based DMS materials, (In,Mn)As and (Ga,Mn)As, is mediated by the mobile holes originating from the magnetic Mn-dopants[1–3]. The ferromagnetic p-type (Ga,Mn)As with a high carrier density (10^{18}–10^{20} cm^{-3}) could possess Curie temperature as high as 110 K.[3] It has also been argued that the Curie temperature of the p-type Mn-doped ZnO semiconductor, with a carrier concentration of 3.5×10^{20} cm^{-3}, could be as high as the room temperature. Recently, these theoretical proposals have stimulated numerous experimental works in an effort to search for high Curie temperature DMS ferromagnets.[4–6] In particular, *ab initio* theoretical calculations predicted a stable ferromagnetic phase in the n-type ZnO with Co doping.[7, 8] Experimentally, significant discrepancies have been reported among different groups and between the measurements and theoretical calculations. The widely proposed mechanism of carrier-induced ferromagnetism in Co-doped ZnO nanowires has not been clarified in the experiment.

ZnO is an oxide semiconductor with a room temperature energy gap of 3.37 eV. In contrast to the other II-VI compound semiconductors, ZnO can be heavily doped with electrons to form a transparent conductor. Since nanostructures are potentially ideal functional components in the future nanometer-scale electronics and optoelectronics, the study of ZnO nanowires is currently of high interest. Realization of spintronic devices from the bottom up would be feasible by adopting the DMS Co-doped ZnO nanowires.[9, 10]

In addition to the carrier concentration, it is theoretically accepted that crystalline quality and structural defects should play an important role in the occurrence and stability of ferromagnetism.[11–13] Thus far, there has been no clear experimental observation to discern this conjecture. In this work, we use natively doped crystalline n-type[14] ZnO nanowires, implanted with Co ions, to investigate the correlations between the structural defects and the strength of ferromagnetism.

ZnO powder was placed in a crucible situated at the center of a quartz tube in a furnace heated to 950°C. A glass substrate at a temperature of 500°C with gold nanoparticles ($\sim$ 40 nm in diameter) as catalysts predeposited on it was located at the downstream end of the quartz tube. The chamber was maintained at 200 Pa with a constant flow of argon. After 8 hours, ZnO nanowires with an average diameter of 40 nm was formed on the glass substrate. The as-grown ZnO nanowires were implanted by Co ions with doses of $(1–6)\times10^{16}$ cm^{-2}. The implantation was performed at room temperature with an accelerating energy of 40 keV by using

*Authors to whom correspondence should be addressed; electronic mail: wbjian@mail.nctu.edu.tw; jjlin@mail.nctu.edu.tw

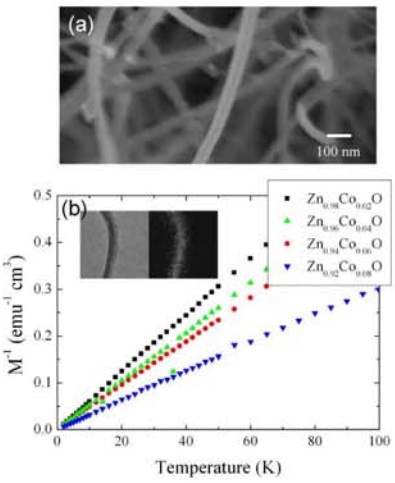

FIG. 1: (a) A typical SEM image of the as-implanted $Zn_{0.94}Co_{0.06}O$ nanowires. (b) The inverse magnetizations of $Zn_{1-x}Co_xO$ nanowires taken at a field of 1000 Oe. The nanowires reveal paramagnetic behavior, and the paramagnetism enhances with increasing Co doping. Insets: An TEM image of a nanowire (left) together with its corresponding EDX mapping image (right) shows an uniform distribution of Co ions in the nanowires.

a tandem accelerator (9SDH-2). The beam current was kept at 150 nA/cm^2 to avoid beam heating. Annealing of the as-implanted ZnO nanowires was then performed at 600°C in a tube furnace under an argon flow of 150 sccm at 1 atm for 12 hours. This annealing temperature would not cause segregation and clustering of the implant ions, as was established previously for ZnO[15] and was confirmed by our HRTEM studies. The annealing at 1 atm prevented any significant change in carrier concentration.[13, 16, 17] Both the as-implanted and annealed ZnO nanowires were characterized by using field-emission scanning electron microscope (JEOL JSM-6330F) and high-resolution transmission electron microscope (JEOL JEM-2010F). Magnetic properties of the nanowires were studied by using a Quantum Design SQUID magnetometer. All the magnetizations as a function of applied field were taken at 2 K.

Most of the ZnO nanowires lay on the substrate with [0001] growth direction in the plane. The high energy Co ions were bombarded on one side of the ZnO nanowires to form DMS nanowires. Computer simulation SRIM code[18] enabled us to estimate the distribution of Co ions in the ZnO nanowires. The Co-ion density distribution as a function of penetration depth showed a peak at 20 nm. The SRIM simulation predicted a range of Co ions about the diameter ($\sim$ 40 nm) of our nanowires.

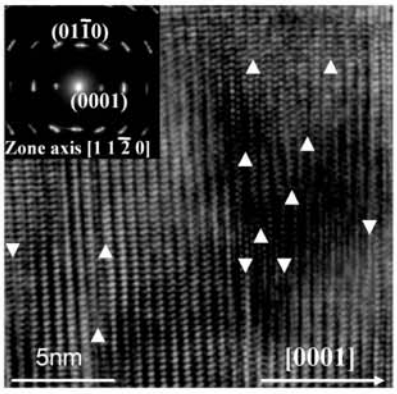

FIG. 2: An HRTEM image of as-implanted $Zn_{0.89}Co_{0.11}O$ nanowires with white triangles indicating stacking faults. Inset: A typical diffraction pattern revealing a rotation of reciprocal lattice points.

Figure 1(a) shows an SEM image of representative as-implanted nanowires. We found that the morphology and dimension of the ZnO nanowires did not change appreciably after implantation, except some slight bending of the nanowires. The energy dispersive X-ray spectroscopy (EDX) compositional map shows Co distribution in the right image of the inset in Fig. 1(b), in comparison to the bright field TEM image in the left. The estimated thickness of a layer of DMS nanowires on the substrate was about 110 nm which was $\sim$ 2 times larger than the estimated ion range by using SRIM code simulation. Figure 1(b) shows a plot of the inverse magnetizations of our $Zn_{1-x}Co_xO$ nanowires with several concentrations x as indicated. These as-implanted nanowires display paramagnetism closely obeying the Curie law. As x increases, the paramagnetism is enhanced, being in accord with the Co concentrations determined from the EDX spectra.

The as-implanted nanowires exhibit paramagnetism, whereas they vaguely reveal ferromagnetic ordering (see squares in Fig. 3(a)). The structural defects produced during the high energy Co-ion bombardment were expected and inspected in detail. The HRTEM image shown in Fig. 2 displays one type of structural defects, i.e., stacking faults, as indicated by the many small triangles. Another type of structural defects is orientation variations. The inset of Fig. 2 shows a typical diffraction pattern of which for the representative as-implanted $Zn_{0.89}Co_{0.11}O$ nanowires. One sees that the lattice planes along the [0001] direction are fairly ordered while there is orientation variation between the $(11\bar{2}0)$ lattice planes. The latter leads to appreciable disorder in the other directions.

Thermal annealing was performed on our nanowires and magnetizations were then remeasured. Figure 3(a)

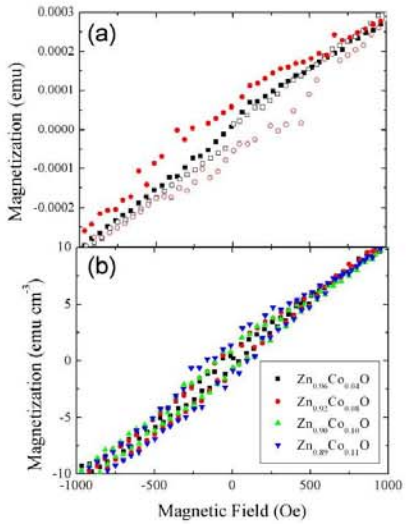

FIG. 3: (a) Magnetization as a function of applied field at 2 K, squares and circles represent as-implanted and annealed $Zn_{0.89}Co_{0.11}O$ nanowires, respectively. (b) Magnetization as a function of applied field at 2 K for annealed $Zn_{1-x}Co_xO$ nanowires with different Co concentrations as indicated. The magnetization for each concentration has been scaled by dividing the factor of its concentration.

shows the field dependent magnetizations of the representative $Zn_{0.89}Co_{0.11}O$ nanowires. The open and closed circles, respectively, stand for the forward and backward sweeping of the magnetic field. For all Co concentrations, the as-implanted nanowires revealed negligible hysteresis while the annealed nanowires displayed distinct ferromagnetism as evidenced in the hysteresis loop (circles in Fig. 3(a)). This comparison study of the as-implanted and annealed samples enable us to identify the mechanism for the enhanced ferromagnetism, i.e., structural defects are detrimental to the occurrence of ferromagnetic ordering. Figure 3(b) shows the magnetizations of $Zn_{0.96}Co_{0.04}O$, $Zn_{0.92}Co_{0.08}O$, $Zn_{0.90}Co_{0.10}O$, and $Zn_{0.89}Co_{0.11}O$ nanowires divided by a factor of 4, 8, 10, and 11, respectively, for comparison. One sees that the hysteresis loops become more profound with increasing Co concentration, implying the formation of domains as well as the enhanced exchange interactions between Co ions. Meanwhile, the magnetization increases with increasing Co-ion implantation, confirming the existence of ferromagnetic, but not previously reported antiferromagnetic[12], order among Co ions.

The structure of the annealed $Zn_{1-x}Co_xO$ nanowires was then inspected by HRTEM. The diffraction pattern

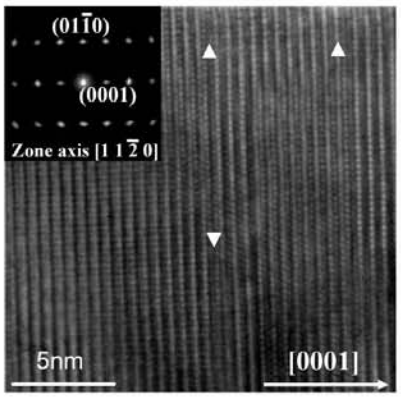

FIG. 4: An HRTEM image of annealed $Zn_{0.89}Co_{0.11}O$ nanowires with white triangles indicating stacking faults. Inset: A typical diffraction pattern showing regular reciprocal lattice points.

in the inset of Fig. 4 clearly shows disappearance of orientation variations. The lattice points along the $[01\bar{1}0]$ direction are now well ordered. Moreover, the HRTEM image of the annealed $Zn_{0.89}Co_{0.11}O$ in Fig. 4 shows a significant reduction in the density of stacking faults. Therefore, it is clear that the improved lattice order in the annealed DMS Co-ZnO nanowires leads to enhanced ferromagnetism. Before annealing, ferromagnetic ordering was deprived due to the presence of a high density of orientation variations and stacking faults. This result strongly suggests that the electron transport with a long mean free path is crucial to the carrier-induced ferromagnetism in Co-ZnO nanowires.

To summarize, 40-nm diameter $Zn_{1-x}Co_xO$ ($x \leq 0.11$) nanowires were synthesized by thermal evaporation, followed by high energy Co-ion implantation. The implanted Co ions were uniformly distributed in the nanowires and they produced many orientation variations and stacking faults as structural defects. After annealing the crystalline lattice order was essentially recovered. The magnetizations then indicated apparent ferromagnetic behavior. This observation is strongly supportive of the current idea of the carrier-mediated ferromagnetism in DMS $Zn_{1-x}Co_xO$ nanowires.

This work was supported by the National Science Council of R.O.C. under Grant Nos. 93-2112-M-009-038 and 93-2120-M-009-009.

[1] T. Dietl, H. Ohno, F. Matsukura, J. Cibert, and D. Ferrand, Science **287**, 1019 (2000).
[2] H. Akai, Phys. Rev. Lett. **81**, 3002 (1998).
[3] F. Matsukura, H. Ohno, A. Shen, and Y. Sugawara,

Phys. Rev. B **57**, R2037 (1998).
[4] K. Ueda, H. Tabata, and T. Kawai, Appl. Phys. Lett. **79**, 988 (2001).
[5] H.-J. Lee, S.-Y. Jeong, C. R. Cho, and C. H. Park, Appl. Phys. Lett. **81**, 4020 (2002).
[6] D. P. Norton, S. J. Pearton, A. F. Hebard, N. Theodoropoulou, L. A. Boatner, and R. G. Wilson, Appl. Phys. Lett. **82**, 239 (2003).
[7] K. Sato and H. Katayama-Yoshida, Jpn. J. Appl. Phys., Part 2 **40**, L334 (2001).
[8] N. A. Spaldin, Phys. Rev. B **69**, 125201 (2004).
[9] Y. Ohno, D. K. Young, B. Beschoten, F. Matsukura, H. Ohno, and D. D. Awschalom, Nature **402**, 790 (1999).
[10] S. A. Wolf, D. D. Awshcalom, R. A. Buhrman, J. M. Daughton, S. von Molnár, M. L. Roukes, A. Y. Chtchelkanova, and D. M. Treger, Science **294**, 1488 (2001).
[11] Y. W. Heo, M. P. Ivill, K. Ip, D. P. Norton, S. J. Pearton, J. G. Kelly, R. Rairigh, A. F. Hebard, and T. Steiner, Appl. Phys. Lett. **84**, 2292 (2004).
[12] A. S. Risbud, N. A. Spaldin, Z. Q. Chen, S. Stemmer, and R. Seshadri, Phys. Rev. B **68**, 205202 (2003).
[13] Y. M. Cho, W. K. Choo, H. Kim, D. Kim, and Y. Ihm, Appl. Phys. Lett. **80**, 3358 (2002).
[14] F. Tuomisto, V. Ranki, K. Saarinen, and D. C. Look, Phys. Rev. Lett. **91**, 205502 (2003).
[15] E. Sonder, R. A. Zuhr, and R. E. Valiga, J. Appl. Phys. **64**, 1140 (1988).
[16] A. Tiwari, C. Jin, J. Narayan, and M. Park, J. Appl. Phys. **96**, 3827 (2004).
[17] C. Ronning, P. X. Gao, Y. Ding, Z. L. Wang, and D. Schwen, Appl. Phys. Lett. **84**, 783 (2004).
[18] J. F. Ziegler and J. P. Biersak, http://www.srim.org.

附錄二： (J. Appl. Phys., to be submitted)

Annealing effects on ferromagnetic properties of Co-implanted ZnO nanowires

Z. Y. Wu, R. T. Huang, F. R. Chen, and J. J. Kai

Department of Engineering and System Science,

National Tsing Hua University, Hsinchu 300, Taiwan ROC

W. B. Jian

Department of Electrophysics, National Chiao Tung University, Hsinchu 300, Taiwan ROC

J. J. Lin

Department of Electrophysics and Institute of Physics,

National Chiao Tung University, Hsinchu 300, Taiwan ROC

Abstract

The $Zn_{1-x}Co_xO$ nanowires with an averaged diameter of $\sim$40 nm have been prepared by thermal evaporation method and then being ion implanted. The as-implanted nanowires were inspected in detail by X-ray diffraction, mapping of electron energy loss spectroscopy, and high resolution transmission electron microscope to make sure that no second phase exists down to a spacial limit of $\sim$1 nm. Two kinds of annealing processes, including annealing under an 1-atm argon flow and that in high vacuum at 600^oC, were performed and their effects on ferromagnetism in $Zn_{1-x}Co_xO$ nanowires were studied. The annealing in an argon flow at 1 atm recovers structural defects of stacking faults and orientation variations, and increases ferromagnetic order. The recovery of crystalline structure has been approved again in the analysis of electron energy loss spectra of Co element in $Zn_{1-x}Co_xO$ nanowires. The second kind of annealing process in high vacuum largely enhances ferromagnetism in $Zn_{1-x}Co_xO$ nanowires. It is suggested that the annealing in high vacuum not only removes structural defects but also increases oxygen vacancies as well as carrier concentration. Both the two kinds of annealing processes enhance ferromagnetic properties of Co-implanted ZnO nanowires.